PHYTOCHROME-DEPENDENT LATE-FLOWERING accelerates flowering through physical interactions with phytochrome B and CONSTANS

Motomu Endo[a,1], Yoshiyasu Tanigawa[a], Tadashi Murakami[b], Takashi Araki[a,1], and Akira Nagatani[b,1]

[a]Graduate School of Biostudies, Kyoto University, Kyoto 606-8501, Japan; and [b]Graduate School of Science, Kyoto University, Kyoto 606-8502, Japan

Edited by Winslow R. Briggs, Carnegie Institution for Science, Stanford, CA, and approved September 20, 2013 (received for review June 4, 2013)

In flowering plants, light is one of the major environmental stimuli that determine the timing of the transition from the vegetative to reproductive phase. In *Arabidopsis*, phytochrome B (phyB); phyA; cryptochrome 2; and FLAVIN-BINDING, KELCH REPEAT, F-BOX 1 are major photoreceptors that regulate flowering. Unlike phyA; cryptochrome 2; and FLAVIN-BINDING, KELCH REPEAT, F-BOX 1, phyB delays flowering mainly by destabilizing the CONSTANS (CO) protein, whose reduction leads to decreased expression of a florigen gene, *FLOWERING LOCUS T*. However, it remains unclear how the phyB-mediated CO destabilization is mechanistically regulated. Here, we identify a unique *PHYTOCHROME-DEPENDENT LATE-FLOWERING* (*PHL*) gene, which is mainly involved in the phyB-dependent regulation of flowering. Plants with mutant *phl* exhibited a late-flowering phenotype, especially under long-day conditions. The late-flowering phenotype of the *phl* mutant was completely overridden by a *phyB* mutation, indicating that PHL normally accelerates flowering by countering the inhibitory effect of phyB on flowering. Accordingly, PHL physically interacted with phyB both in vitro and in vivo in a red light-dependent manner. Furthermore, in the presence of phyB under red light, PHL interacted with CO as well. Taken together, we propose that PHL regulates photoperiodic flowering by forming a phyB–PHL–CO tripartite complex.

light signaling | FT

In plants, light is used not only as an energy source but as a signal to sense and adapt to the surrounding environment. Among various environmental stimuli, including biotic stress, temperature, and nutrition, light plays a pivotal role in the life cycle of plants; flowering control is no exception (1). In *Arabidopsis,* light perception is mediated by the red/far-red light-receptor and blue light-receptor phytochromes (phyA–E). Phytochromes can exist in two distinct forms, red-light-abosrobing state (Pr) and far-red-light-absorbing state (Pfr), depending on the light quality. Red light activates phytochromes by converting Pr to Pfr, whereas far-red light decreases the level of the active form by converting Pfr back to Pr. The blue/UV-A light-receptor cryptochromes (cry1, cry2); phototropins (phot1, phot2); FLAVIN-BINDING, KELCH REPEAT, F-BOX 1 (FKF1); and the UV-B receptor UV RESISTANCE LOCUS 8 (2–6) are also important for light signaling.

The aforementioned photoreceptors phyB, phyA, cry2, and FKF1 transcriptionally regulate the expression of a key flowering factor CONSTANS (CO). In *Arabidopsis*, the level of *CO* mRNA is regulated by the circadian clock, resulting in peak *CO* expression at night (7). Red light and blue light play antagonistic roles in the regulation of *CO* mRNA transcription. In response to red light, phyB down-regulates *CO* mRNA transcription through factors such as PHYTOCHROME AND FLOWERING TIME 1 (8–10). In contrast, cry2 and phyA up-regulate *CO* mRNA transcription (7, 11). FKF1 also up-regulates *CO* mRNA transcription by degrading CYCLING DOF FACTORs in response to blue light (12).

Equally important is the regulation of CO protein stability (13). Observations of mutant phenotypes have established that phyB destabilizes CO protein, whereas phyA, cryptochromes, and FKF1 stabilize it in the long-day afternoon (13, 14). Recently, HIGH EXPRESSION OF OSOTICALLY RESPONSIVE GENES 1 (HOS1), an E3 ubiquitin ligase, was demonstrated to be involved in ubiquitination of CO protein during the day, whereas CONSTITUTIVE PHOTOMORPHOGENIC 1 (COP1) is involved in degradation of CO at night (15, 16). CO is degraded in the morning independent of COP1 by a phyB-dependent mechanism, and a ubiquitin ligase, such as HOS1, might be involved in that process (15, 17).

The elevation in the level of CO protein, in turn, up-regulates the expression of *FLOWERING LOCUS T* (*FT*), which encodes the mobile florigen (18–20). Consequently, expression of another flowering regulator, *SUPPRESSOR OF OVEREXPRESSION OF CO 1* (*SOC1*), is regulated by *FT* (21–23). Consistent with the flowering phenotype, expression levels of *FT* and *SOC1* are increased in the *phyB* mutant, whereas they are reduced in the *cry2* mutant (7, 9).

Here, we identified a *PHYTOCHROME-DEPENDENT LATE-FLOWERING* (*PHL*) gene encoding a nuclear protein with a glutamine-rich region. PHL accelerates flowering by suppressing the inhibitory effect of phyB on flowering. Furthermore, a tripartite complex consisting of phyB, PHL, and CO forms in a red light-dependent manner. On the basis of these findings, we propose a model explaining how such a complex is involved in the photoperiodic regulation of flowering.

Results

Isolation and Molecular Characterization of Mutants Deficient in At1g72390. The At1g72390 gene was originally isolated as a candidate for a phototropin interacting factor by yeast two-hybrid screening (Fig. S1). However, a recessive mutant strain generated

Significance

In plants, red light and blue light have antagonistic functions for the regulation of a flowering activator, CONSTANS (CO). Recently, direct regulation of CO by blue light photoreceptors has been reported. However, how red light regulates CO has remained unclear. In this paper, we identify a novel *PHYTOCHROME-DEPENDENT LATE-FLOWERING* (*PHL*) gene directly involved in red light photoreceptor phytochrome B (phyB) signaling. Furthermore, we reveal that PHL can bridge phyB and CO in a red light-dependent manner. These findings provide insight into the coordinated regulation of CO by red and blue photoreceptors in flowering regulation. Because PHL homologues are found in a wide variety of plant species, the mechanism we propose here appears to be universal to all flowering plants.

Author contributions: M.E. and A.N. designed research; M.E., Y.T., and T.M. performed research; and M.E., T.A., and A.N. wrote the paper.

The authors declare no conflict of interest.

This article is a PNAS Direct Submission.

[1]To whom correspondence may be addressed. E-mail: moendo@lif.kyoto-u.ac.jp, taraqui@lif.kyoto-u.ac.jp, or nagatani@physiol.bot.kyoto-u.ac.jp.

This article contains supporting information online at www.pnas.org/lookup/suppl/doi:10.1073/pnas.1310631110/-/DCSupplemental.

by a transferred DNA (T-DNA) insertion in the At1g72390 gene (SALK_017615) did not display phototropism and a chloroplast relocation phenotype (Fig. S2). Instead, the mutant exhibited a late-flowering phenotype under long-day (LD) conditions (Fig. 1 *A*, *D*, and *F*).

To confirm that the mutation in the At1g72390 gene indeed caused the late-flowering phenotype, we isolated another allele containing a single base substitution in At1g72390, by the targeting induced local lesions in genomes (TILLING) method (24) (Fig. 1*B*). The mutation was a single Ala-to-Val amino acid substitution (A1026V), and the mutant exhibited the late-flowering phenotype under LD conditions, as expected (Fig. 1 *A* and *D*). Hereafter, the At1g72390 gene is referred to as *PHL* after its flowering-time phenotype (the relationship with phyB is discussed below). Accordingly, the T-DNA–tagged and single-base substitution mutants are referred to as *phl-1* and *phl-2*, respectively (Fig. 1*B*).

To confirm further that *PHL* was the causal gene for the late-flowering phenotype, we established several transgenic lines that expressed *PHL* fused to the β-glucuronidase (GUS) gene driven by the authentic *PHL* promoter in the *phl-1* mutant background (PHLpro:PHL-GUS *phl-1*). The levels of *PHL* mRNA in the WT and those of *PHL-GUS* mRNA in PHLpro:PHL-GUS *phl-1* no. 2 and no. 3 were analyzed by quantitative RT-PCR (qPCR), and they were comparable to each other (Fig. 1*C*). Flowering time under LD conditions was also comparable to WT, indicating that the *PHL-GUS* gene was able to complement the late-flowering phenotype of the *phl-1* (Fig. 1 *A*, *C*, and *D*). We also prepared transgenic lines that overexpressed PHL fused to a T7 tag, under control of the cauliflower mosaic virus (CaMV) 35S promoter in a WT background, referred to as PHLox. The PHLox line produced a 100-fold elevated *PHL* mRNA level and showed a slightly early-flowering phenotype under LD conditions (Fig. 1 *A*, *C*, and *D*). We therefore concluded that the mutations in the *PHL* gene are indeed responsible for the late-flowering phenotype of the *phl* mutant plants.

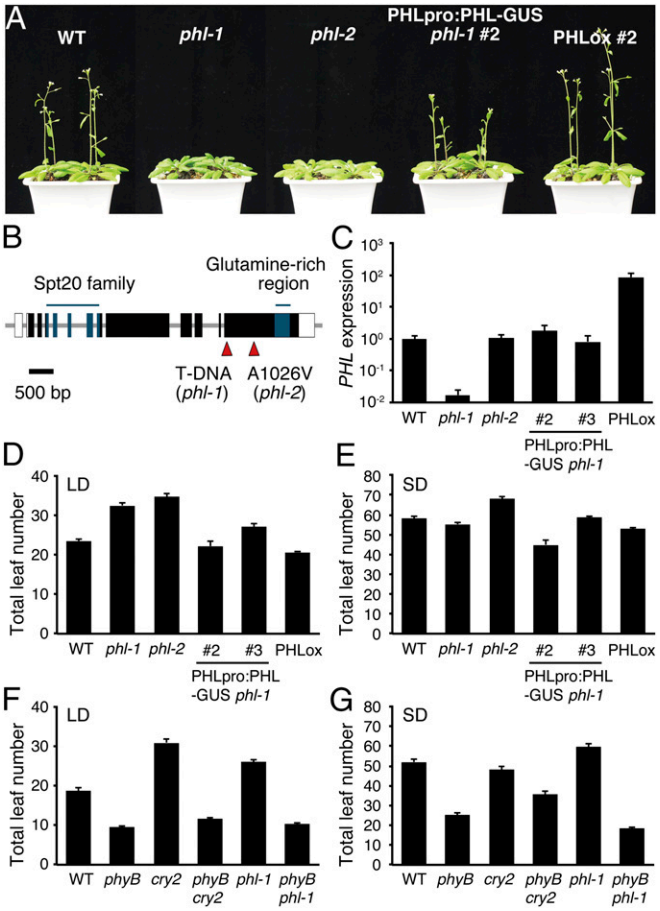

Fig. 1. Structure of the *PHL* gene and flowering phenotype of the *phl* mutants. (*A*) Flowering phenotype of the *phl* mutants and complementation lines. Plants were grown under LD conditions for 3 wk. (*B*) Structure of the *PHL* gene [Arabidopsis Genome Initiative (AGI) code At1g72390]. Boxes and lines represent exons and introns, respectively. Open boxes illustrate 5′- and 3′-untranslated regions, black boxes illustrate the coding region, and the Spt20 family domain and a glutamine-rich region are shown as bars. The positions of mutations are indicated with red triangles. (*C*) Relative *PHL* mRNA expression in seedlings. Plants were grown under LD conditions for 10 d. *ISOPENTENYL PYROPHOSPHATE:DIMETHYLALLYL PYROPHOSPHATE ISOMERASE 2* (*IPP2*) was used as an internal control. Data were normalized to the *PHL* level in WT. Mean ± SEM ($n = 3$). Plants were grown under LD (*D* and *E*) and SD (*F*) conditions. Mean ± SEM ($n \geq 15$).

The *PHL* encodes a polypeptide of 1,325 aa residues with no similarity to other proteins in the *Arabidopsis* genome. It was annotated as a hypothetical protein (www.ncbi.nlm.nih.gov/gene/843571) that contains an InterPro domain (Spt20 family) in its N terminus (61–203 aa) and a glutamine-rich region in its C terminus (1,160–1,265 aa) (Fig. 1*B*).

Genetic and Physiological Analyses on the Late-Flowering Phenotype in *phl*. The *phl-1* and *phl-2* mutants flowered substantially later under LD conditions but almost normally under short-day (SD) conditions (Fig. 1 *D* and *E*), indicating that the effect of PHL on flowering depended on the photoperiod. This characteristic is reminiscent of photoperiod pathway mutants, such as *cry2*, *ft*, and *co*, all of which show more severe late-flowering phenotypes under LD than SD conditions (25).

We then observed the flowering phenotype of the *phl-1* mutation crossed into a photoreceptor mutant background under different light conditions. The late-flowering phenotype of the *phl-1* mutant was completely overridden by the *phyB* mutation (*phl-1* vs. *phyB phl-1*) (Fig. 1 *F* and *G*). A similar strong dependency of cry2 on phyB has been reported (26). Hence, as is the case with cry2, PHL appears to accelerate flowering by suppressing phyB activity.

To examine the functional relationship between different photoreceptors and PHL further, we observed the flowering phenotype under continuous red light (cR), where phyB is maximally activated but cry2 remains inactive. Accordingly, the *cry2* mutant did not show a late-flowering phenotype under this condition (Fig. S3*A*). Nevertheless, the *phl-1* mutant exhibited a weak but statistically significant late-flowering phenotype, indicating that PHL could affect flowering in the absence of cry2 activation. Furthermore, this phenotype was completely overridden in the *phyB* mutant background (*phl-1* vs. *phyB phl-1*), suggesting that PHL accelerates flowering by suppressing the activity of phyB.

Under continuous blue light (cB), cryptochromes are fully activated and phyB is partially activated. Consequently, WT, *cry2*, and *phyB* flower equally early (26). Hence, no sole photoreceptor dominates the flowering under this condition. Nevertheless, the *phl*-1 mutant exhibited a weak but statistically significant late-flowering phenotype (Fig. S3*B*). Importantly, this phenotype was completely overridden in the *phyB* mutant background (*phl-1* vs. *phyB phl-1*), suggesting that PHL accelerated the flowering by suppressing the activity of phyB even under cB.

Because photoreceptors regulate various physiological responses other than flowering (27), we examined the hypocotyl elongation and cotyledon expansion responses in the *phl* mutant under cR, cB, and continuous far-red light (cFr) conditions (Figs. S4 and S5). Although the hypocotyl was slightly longer in the *phl-1* mutant than in WT under cR, the hypocotyl length and cotyledon area in the mutant were almost indistinguishable from those of the other lines under cR, cB, and cFr. Hence, PHL appeared to be a modulator of phyB specific to flowering.

Effects of PHL on the Expression of Flowering-Related Factors. Because PHL appears to function in the photoperiod pathway of flowering (Figs. 1 and 2), we first examined if PHL affected mRNA levels of the major photoreceptors. Using qPCR, we

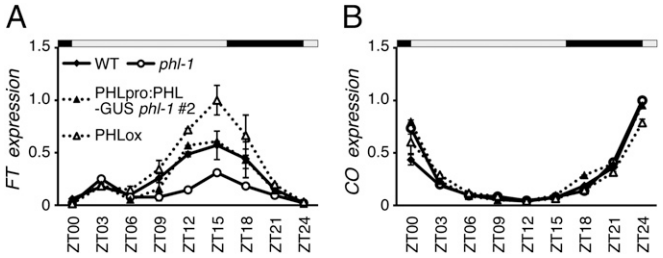

Fig. 2. Diurnal expression of *FT* and *CO* in the *phl* mutants. Seedlings were grown under LD conditions for 9 d, and RNA was then extracted from seedlings every 3 h over a 24-h period in LD conditions. *IPP2* was used as an internal control to determine relative levels of *FT* (*A*) and *CO* (*B*) mRNA. Open bars indicate light intervals, and closed bars indicate dark intervals. Mean ± SEM ($n = 3$).

detected normal levels of *PHYB* and *CRY2* mRNA in the *phl-1* mutant (Fig. S6*A*). We next examined the abundance of phyB and cry2 proteins under LD conditions in the *phl-1* mutant by Western blot assay. The amounts of both proteins were comparable to those in WT (Fig. S6*B*). Hence, PHL appeared to affect the signaling processes downstream of photoreceptors rather than photoreceptors themselves.

Light signals from multiple photoreceptors are integrated into the flowering pathway consisting of key factors, such as *CO*, *FT*, *TWIN SISTER OF FT* (*TSF*), *SOC1*, and *FLOWERING LOCUS C* (*FLC*) (8, 21, 22, 28–30). In the early-flowering *phyB* mutant, expression of *FT, TSF*, and *SOC1* is increased (9, 22). By contrast, *FT* expression is reduced in the late-flowering *cry2* mutants (7). We thus examined the levels of *FT*, *SOC1*, *CO*, and *FLC* expression in WT, *phl-1*, PHLpro:PHL-GUS *phl-1* no. 2, and PHLox over the course of a day under LD conditions (Fig. 2 and Fig. S7).

In the *phl-1* mutant, *FT* expression was substantially reduced compared with WT, which was consistent with the late-flowering phenotype in the mutants (Fig. 1). *SOC1* expression was reduced as well. Furthermore, their expression was fully restored in the PHLpro:PHL-GUS *phl-1* no. 2 and PHLox strains. By contrast, the expression levels of *CO* and *FLC* were unaffected by the *phl* mutation.

Many photoperiod pathway-related genes exhibit diurnal oscillation of gene expression, and proper oscillation of transcripts or products is important for their functions (31). Indeed, the *FT*, *SOC1*, *CO*, and *FLC* expression exhibited diurnal oscillation under LD conditions, whereas the phase of the oscillation was not affected by the *phl-1* mutation (Fig. 2 and Fig. S7). Hence, we concluded that the late-flowering phenotype in the *phl* mutants was caused by the reduction in the expression levels of *FT* and *SOC1* rather than a phase shift in the diurnal oscillation.

Physical Interaction Between PHL and phyB. As shown above, PHL appeared to accelerate flowering by inhibiting phyB activity. This prompted us to ask whether the PHL protein physically interacted with phyB. First, we compared the intracellular localization patterns of the PHL-YFP fusion protein with those of phyB-GFP that were previously reported (32, 33). Plasmids harboring 35S:PHL-YFP were transformed into tobacco (*Nicotiana bethamiana*) epidermal cells by agrobacterium infiltration, and YFP fluorescence was observed. PHL-YFP fluorescence was uniformly detected in the nuclei, and nuclear bodies were occasionally observed (Fig. 3*A*). In addition, PHL-YFP formed cytoplasmic granules in some cells. This raised the possibility that PHL and phyB might colocalize, at least in the nucleus.

We tested the direct interaction between phyB and PHL in yeast cells. In the yeast two-hybrid assay, phyB interacted with the N terminus of PHL (Fig. 3*B*), although interaction with the full length of PHL and C terminus of PHL was not detected (Fig. 3*B*). We then performed a bimolecular fluorescence complementation (BiFC) analysis in plant cells. The N-terminal half of YFP (YN) was fused to PHL, and the C-terminal half of YFP (YC) was fused to phyB, and both constructs were transiently expressed in tobacco. Reconstituted YFP fluorescence was observed in the nucleus, indicating that phyB interacts with PHL in the nucleus *in planta* (Fig. 3*C* and Table S1).

To investigate the PHL–PhyB interaction further, a coimmunoprecipitation assay was carried out under red and far-red light conditions to see if the interaction depends on the light condition. PHL-T7–, phyB-GFP–, and GFP-clarified whole-cell extracts were separately prepared from PHLox, PBG18 (34), and 35S:GFP (35) plants, respectively, and combinations of extracts were pooled before immunoprecipitation. As expected, PHL-T7 was immunoprecipitated with anti-T7 antibody. Furthermore, phyB-GFP was coimmunoprecipitated with PHL only under red light conditions (Fig. 3*D*), indicating that phyB interacts with PHL in a Pfr-dependent manner.

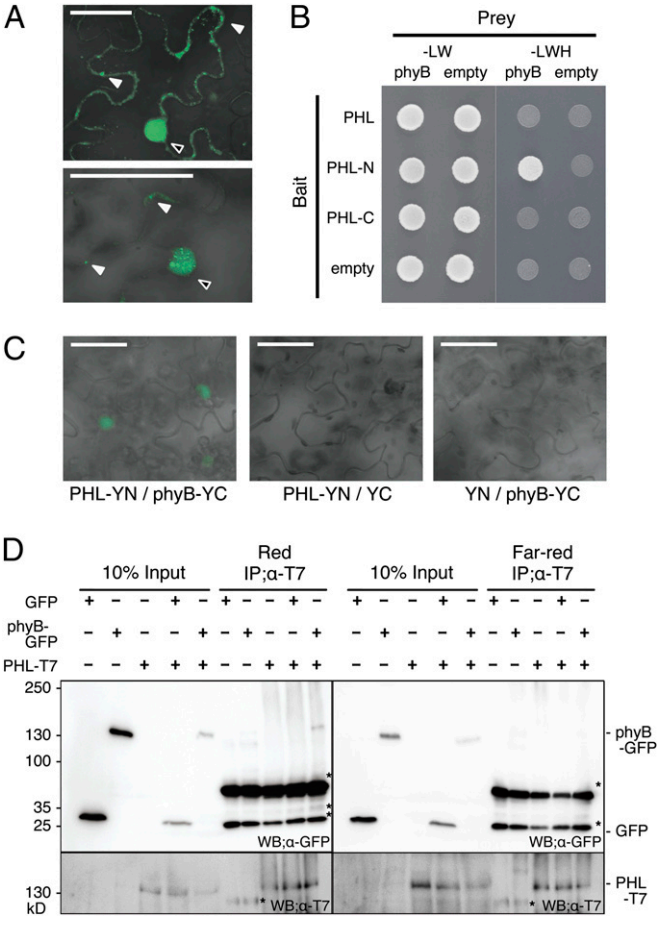

Fig. 3. Direct interaction of PHL with phyB. (*A*) PHL-YFP fluorescence in tobacco leaf epidermal cells grown under 16-h red light and 8-h dark conditions. Enhanced YFP (EYFP) fluorescence and a bright-field image were merged. A solid arrowhead and open arrowhead indicate EYFP fluorescence in a nucleus and cytoplasmic granule, respectively. (*Lower*) Nuclear bodies were observed in the nucleus. (Scale bar = 100 μm.) (*B*) Interaction between PHYB and the N terminus of PHL was tested by the yeast two-hybrid assay. Yeast cells transformed with the indicated combination of plasmids were spotted onto an Sc–Leu–Trp plate (–LW) or an SC–Leu–Trp–His plate (–LWH). (*C*) BiFC analysis of the interaction between phyB and PHL in tobacco leaf epidermal cells grown under 16-h red light and 8-h dark conditions. EYFP fluorescence and a bright-field image were merged. (Scale bar = 100 μm.) (*D*) PHL-T7 and phyB-GFP were tested by a coimmunoprecepitation assay. Proteins extracted from plants were mixed, incubated under red/far-red light, and coimmunoprecipitated using anti-T7 antibody. The bound proteins eluted from the beads were then subjected to immunoblot analysis. The Western blots (WB) were probed with an anti-GFP antibody (WB; α-GFP) and with an anti-T7 antibody (WB; α-T7). The asterisk indicates nonspecific bands.

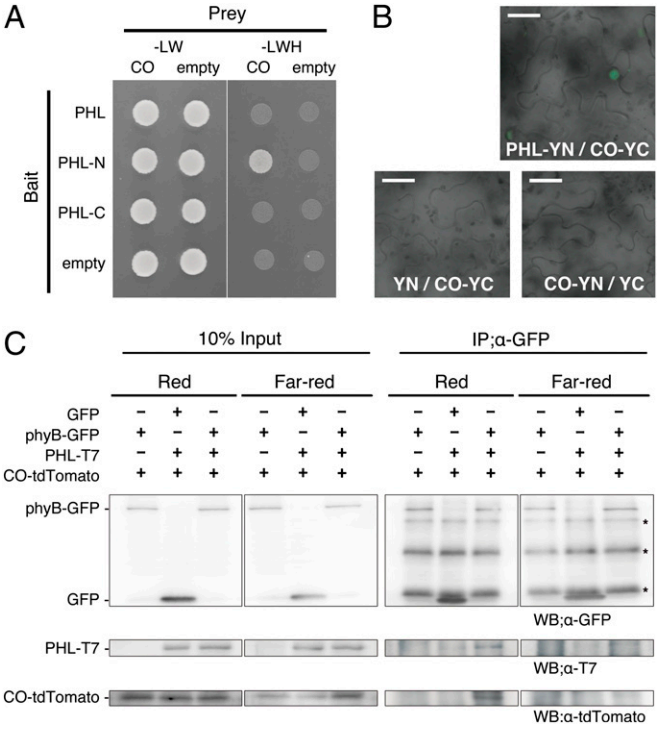

Fig. 4. Direct interaction of PHL with CO. (*A*) Interaction between CO and the N terminus of PHL was tested by the yeast two-hybrid assay. Yeast cells transformed with the indicated combinations of plasmids were spotted onto an Sc−Leu−Trp plate (−LW) or an SC−Leu−Trp−His plate (−LWH). (*B*) BiFC analysis of the interaction between PHL and CO in tobacco leaf epidermal cells under continuous white light conditions. Enhanced YFP (EYFP) fluorescence and a bright-field image were merged. (Scale bar = 100 μm.) (*C*) Interaction between phyB, CO, and PHL in an immunoprecipitation assay. CO-tdTomato, PHL-T7, and phyB-GFP were tested by a coimmunoprecipitation assay. Proteins extracted from plants were mixed under white light conditions, incubated under red/far-red light, and coimmunoprecipitated using anti-GFP antibody. The bound proteins eluted from the beads were then subjected to immunoblot analysis. The blots were probed with an anti-GFP antibody (WB; α-GFP), anti-RFP antibody (WB; α-tdTomato), and anti-T7 antibody (WB; α-T7). The asterisk indicates nonspecific bands.

Tripartite Complex Consisting of PHL, CO, and phyB. As shown above, PHL probably interacts with phyB to suppress the activity of phyB on CO. The main mechanism by which phyB affects flowering is light-dependent destabilization of the CO protein (13). Although no physical interaction or colocalization between phyB and CO has been reported, we posited that PHL might interact with both of them. To test this possibility, we carried out a yeast two-hybrid assay. We observed an interaction between full-length CO and the N terminus of PHL (Fig. 4*A*). To confirm whether full-length PHL directly interacts with CO in plant cells, a BiFC assay in tobacco epidermal cells was performed. Fluorescence derived from the combination of PHL-YN and CO-YC was observed in the nucleus, suggesting that PHL can interact with CO directly *in planta* (Fig. 4*B* and Table S1).

To examine if phyB, PHL, and CO could form a tripartite complex, a coimmunoprecipitation assay was performed. PHL-T7– phyB-GFP– and GFP-clarified whole-cell extracts were separately prepared from PHLox, PBG18, and 35S:GFP strains, respectively. Extracts containing CO-tdTomato were prepared from tobacco leaves that transiently expressed CO-tdTomato under the CaMV 35S promoter, and combinations of extracts were mixed before immunoprecipitation. The phyB-GFP or GFP was then immunoprecipitated with anti-GFP antibody under red and far-red light conditions. Consequently, PHL-T7 and CO-tdTomato were coimmunoprecipitated with phyB-GFP only under red light, consistent with the notion that a phyB–PHL–CO tripartite complex was formed in a Pfr-dependent manner (Fig. 4*C*).

Expression Patterns of the *PHL* Transcripts and the PHL Protein. We next sought to determine which organs/tissues expressed *PHL*. For this purpose, qPCR analysis was performed on 10-d-old seedlings grown under continuous white light. Although *PHL* mRNA was detectable in all organs examined, it was more abundant in cotyledons. In leaves, the *PHL* mRNA was detected both in mesophyll and vasculature cells (Fig. S8*A*). Many genes involved in photoperiodic regulation exhibit diurnal oscillation with respect to their gene expression. Hence, the diurnal change of *PHL* expression levels under LD conditions was measured by qPCR. However, the expression level did not fluctuate over time, suggesting that *PHL* mRNA levels are not clock-regulated (Fig. S8*B*).

Protein levels in the key regulatory factors of photoperiodic flowering also diurnally oscillate. Hence, we examined whether the protein levels of PHL varied throughout the day. For this purpose, a plasmid harboring 35S:PHL-YFP was transformed into tobacco epidermal cells transiently and the fluorescence of PHL-YFP was observed under LD conditions (Fig. 5).

Under LD conditions, nuclear localization of the PHL-YFP fusion protein was scarcely observed, and PHL-YFP was mainly localized in the cytoplasm and cytoplasmic granules during the night period [zeitgeber time (ZT)16.5, ZT20, and ZT23.5]. In the morning (ZT0.5 and ZT4), PHL-YFP fluorescence in the cytoplasm disappeared and nuclear fluorescence began to appear. Cytoplasmic granules of PHL-YFP still existed. At ZT8 and ZT12, clear accumulation of PHL-YFP in the nucleus was observed. Similar results were obtained under SD conditions (Fig. S9), implying that the abundance of PHL in the nucleus was posttranscriptionally regulated by the circadian clock but not directly by light.

Discussion

Functional Dependence of PHL on phyB. The late-flowering phenotype of the *phl* mutant was completely overridden by a *phyB* mutation under all the light conditions tested (Fig. 2). The *phl* mutant resembles the *cry2* mutant in this regard (26). Hence, PHL, as is the case with cry2, appears to accelerate flowering by suppressing the inhibitory effect of phyB on flowering. Signals from multiple photoreceptors, such as phyB, phyA, cry2, and FKF1, are known to be integrated to regulate the levels of CO for flowering regulation (13, 14, 16). Similarly, PHL might accelerate flowering by stabilizing the CO protein. The observation that the *cry2 phl-1* double mutant did not flower later than the respective single mutants further supports this idea (Fig. S3).

Many genes are identified as factors involved in phyB signaling. The majority of respective mutants have a photomorphogenic phenotype in seedlings, such as de-etiolation, hypocotyl elongation, and cotyledon expansion (36). By contrast, the *phl*

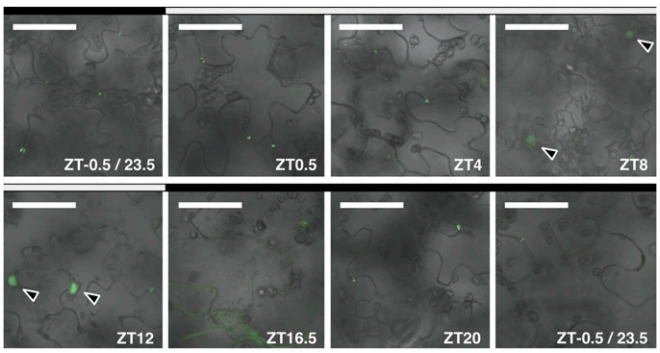

Fig. 5. Subcellular localization of PHL-YFP. PHL-YFP fluorescence in tobacco leaf epidermal cells incubated under LD conditions was tested. EYFP fluorescence and a bright-field image were merged. Arrowheads indicate EYFP fluorescence in the nucleus. Bars at top represent diurnal cycle (light, white box; dark, black box). (Scale bar = 100 μm.)

mutants did not exhibit a clear phenotype in hypocotyl elongation and cotyledon expansion (Figs. S4 and S5). These observations lead us to expect that there are specific genes downstream of phyB that are involved in distinct phenomena, such as hypocotyl elongation or flowering. This view is further supported by the fact that the mutants of PHYTOCHROME-INTERACTING FACTORs (PIFs) did not show an aberrant flowering phenotype (37). Furthermore, genes in the phyB signaling pathway that exclusively affect flowering are rather scarce, suggesting that only a small number of genes link phyB to flowering pathway integrators, such as *FT* and *SOC1* in the signal transduction pathway. This is consistent with our result that PHL directly bridges phyB and CO.

Direct Interaction of PHL with phyB and CO. We demonstrated that PHL physically interacts with phyB in vitro and in vivo (Fig. 3). Furthermore, both PHL and phyB are localized to the nucleus and formed nuclear bodies (Fig. 3*A*). These observations are consistent with the fact that the *phl-1* phenotype was observed under cR and was completely overridden by the *phyB* mutation (Fig. S3*A*). PHL-YFP was localized mainly in the nucleus, but some portion was observed in the cytoplasm and cytoplasmic granules (Figs. 3*A* and 5 and Fig. S9). Nuclear fluorescence was observed in the BiFC assay, suggesting the importance of PHL in the nucleus for flowering regulation (Fig. 3*C*).

We also showed that a phyB–PHL–CO complex was detected in a red light-specific manner (Fig. 4*C*). Hence, it is more likely that PHL regulates CO protein stability rather than its transcription. Consistent with this view, type II phytochromes (mainly phyB) are shown to regulate CO protein stability (13, 17), although phyB is also known to regulate *CO* mRNA levels as well (8, 9). As we previously reported, photoreceptors, including phyB, have tissue specificity for flowering regulation (38–40). Dual regulation by one factor is also seen in a blue-light receptor FKF1, which regulates both *CO* mRNA and CO protein stability by different mechanisms (12, 14). In this regard, PHL might specifically suppress phyB function in vasculature. It is important to elucidate the site of PHL action at the tissue level in future studies.

Diurnal Change in Nuclear Levels of PHL. The *PHL* mRNA has no rhythmic oscillation throughout the day. Nevertheless, PHL-YFP protein expressed under the control of the constitutive 35S promoter gradually accumulated in the nucleus during the daytime and disappeared from the nucleus at around ZT16 (Fig. 5). This suggests nuclear PHL protein abundance is regulated posttranscriptionally. A well-characterized phyB interactor, PIF3, is mainly required for phytochrome signaling during de-etiolation, and it is degraded in a red light-dependent manner within an hour (41). The degradation of PIF3 is regulated by COP1 (42). CO protein is also quickly degraded by COP1 after the onset of the night period, whereas CO protein is slowly degraded in the morning independent of COP1 (13, 17). A recent report suggests that HOS1, another E3 ubiquitin ligase, is involved in CO protein degradation in the morning (15). Likewise, PHL protein might be degraded by COP1 rather than HOS1 in the nucleus as is the case with CO.

PHL-YFP also localized to cytoplasmic granules (Figs. 3*A* and 5 and Fig. S9). Recently, it was reported that phytochrome regulates translation of mRNA in the cytosol (42). In this study, we have not shown that phyB interacts with PHL in cytoplasmic granules, but this possibility should be explored in future studies.

Molecular Nature of PHL. *PHL* orthologs were found at least in eudicots (20 species, including *Arabidopsis lyrata*, *Medicago sativa, Solanum lycopersicum*, and *Populus trichocarpa*), monocots (5 species, including *Oryza sativa*), and a gymnosperm (*Cryptomeria japonica*), whereas they were not found in lycopodiophytes (*Selaginella moellendorffii*), moss (*Physcomitrella patens*), and chlorophytes (*Chlamydomonas reinhardtii* and *Ostreococcus lucimarinus*). Those plant species include not only LD but SD and day-neutral plants. Hence, PHL might regulate flowering not only in LD plants. However, this should be experimentally verified in future studies.

PHL contains an InterPro domain, Spt20 family, in its N terminus. Spt20/ADA5 is known as a member of the Spt-Ada-Gcn5-Acetyltransferase (SAGA) complex, which mediates histone deacetylation (43). In *Arabidopsis*, Spt20/ADA5 orthologs are not well characterized, but Spt20/ADA5 is involved in maintaining the integrity of the SAGA complex in yeast and humans (44, 45). PHL also contains a glutamine-rich region in its C terminus, which potentially functions as a type of transcriptional coactivator (46). Furthermore, recent reports have illustrated that coactivators have pleiotropic roles not related to transcription. Peroxisome proliferator-activated receptor γ coactivator-1α is a well-characterized transcription coactivator in mammals. Such coactivators are highly responsive to a variety of environmental cues, ranging from temperature to nutritional status, and they coordinately regulate metabolic pathways and biological processes in a tissue-specific manner (47).

The phenotypes of these mutants suggest that PHL is more likely to regulate CO protein accumulation than to regulate CO function. Hence, PHL is assumed to be a suppressor of phyB signaling rather than a transcriptional coactivator.

Possible Mechanisms of PHL Action. In this study, we showed that PHL protein is a unique interactor that bridges phyB and CO protein. Here, we show a working model depicting the possible functional relationship of phyB, PHL, and CO for *FT* regulation under LD conditions (Fig. 6).

The half-life of the Pfr form of phyB is substantially longer than the dark period length of LD conditions (48). Hence, almost all phyB is in the Pfr form throughout the day. Nevertheless, the stability of CO protein diurnally changes (13). Genetic analysis and direct interactions suggest that PHL functions as a suppressor of CO degradation by phyB through the red light-specific interaction. Hence, PHL, whose nuclear levels exhibited diurnal change (Fig. 6), might determine when in the day CO accumulates. In the current model, phyB degrades CO protein in the morning, whereas cry2 and FKF1 stabilize CO in the afternoon to accelerate flowering (14, 16). For this purpose, the plant should accumulate CO at a certain level before the afternoon. Because PHL is a suppressor of phyB, it would help CO to reach such a level. By means of this mechanism, PHL would fine-tune how plants respond to the day length for the regulation of flowering. Thus, a phyB–PHL complex balances CO protein levels to achieve appropriate photoperiodic flowering in *Arabidopsis*.

In conclusion, we propose that PHL suppresses phyB-dependent CO protein degradation, especially in the LD afternoon in the presence of cry2 and FKF1. The observation of CO protein

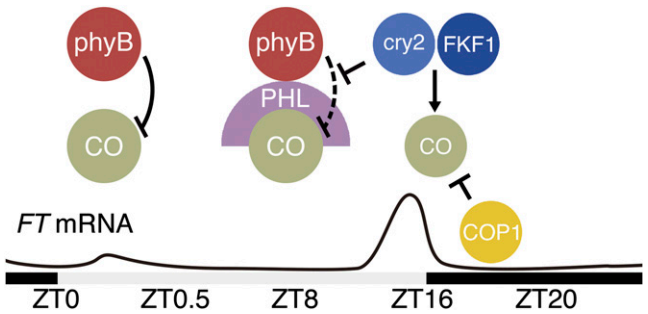

Fig. 6. Working model of PHL for flowering regulation. High abundance of PHL in the nucleus in the afternoon suppresses phyB-dependent CO protein degradation by interacting with the Pfr form of phyB and CO. In combination with COP1-dependent CO degradation and blue light-dependent stabilization of CO protein by cry2 and FKF1, CO protein abundance is regulated as previously shown (13). cry2 function as a suppressor of phyB signaling is observed as previously shown (26). PHL interacts with both phyB and CO in a red light-dependent manner, and the tripartite complex in the afternoon induces *FT* mRNA expression depicted by the black curve. Open bars indicate light intervals, and closed bars indicate dark intervals.

abundance in the *phl* mutant will be studied in the future to identify how PHL suppresses CO protein degradation.

Materials and Methods

Plant Materials and Growth Conditions. WT *Arabidopsis thaliana* and all the *Arabidopsis* mutants used were in the Columbia (Col-0) ecotype background. The *phl-1* (SALK_017615) was obtained from the SALK T-DNA insertion collection (http://signal.salk.edu/) and backcrossed three times before the analysis. The *phl-2* (A1026V) allele was obtained from the Seattle TILLING project (http://tilling.fhcrc.org/) and backcrossed three times. The *phyB-9* (CS6217; *Arabidopsis* Biological Resource Center) and *cry2-2* (11) strains were also used.

Plants grown in LD conditions (16 h of white light at ~35 $\mu mol \cdot m^{-2} \cdot s^{-1}$, 8 h of darkness) and SD conditions (8 h of white light at ~70 $\mu mol \cdot m^{-2} \cdot s^{-1}$, 16 h of darkness) received the same total fluorescence of light. For the analyses under continuous light conditions, plants were grown under continuous blue LED [100 $\mu mol \cdot m^{-2} \cdot s^{-1}$ (470 ± 13 nm)], red LED [100 $\mu mol \cdot m^{-2} \cdot s^{-1}$ (660 ± 13 nm)], or white light (~50 $\mu mol \cdot m^{-2} \cdot s^{-1}$ from fluorescent light tubes). Hypocotyl lengths and cotyledon area were measured using ImageJ software (National Institutes of Health).

Coimmunoprecipitation Assay. For phyB-GFP and GFP, PBG18 and 35S:GFP plants were grown for 10 d under LD conditions. For CO-tdTomato, pPZP211/35S:CO-tdTomato was agroinfiltrated into *N. benthamiana* and incubated for 36 h under continuous white light conditions. For PHL-T7, etiolated PHLox seedlings were grown under dark conditions for 7 d. Proteins were extracted as previously described (49). Proteins were then mixed under white light conditions and incubated for 4 h under red and far-red light conditions. PHL-T7 and phyB-GFP were coimmunoprecipitated by using anti-T7 antibody (no. 69522; Novagen) and anti-GFP antibody (04404-84; Nacalai Tesque), respectively, and Dynabeads Protein G (Dynal). Bound proteins were eluted; fractionated by 7.5% (vol/vol) and 12.5% (vol/vol) SDS-PAGE; and subjected to protein gel blot analysis using anti-GFP antibody, anti-RFP antibody (M165-3; MBL), and anti-T7 antibody. Other methods are described in *SI Materials and Methods*.

ACKNOWLEDGMENTS. We thank T. Koto and H. Shimizu for technical assistance, D. Baulcombe for providing *p19* silencing suppressor, T. Nishimura for providing the pPZP211/NP vector, C. Lin for providing anti-cry2 antibody, and J. A. Hejna for English proofreading. This work was partially supported by Grant-in-Aid for Scientific Research (B) 17370018 (to A.N.); Grants-in-Aid for Scientific Research on Priority Areas 17084002 (to A.N.), and 19060012 and 19060016 (to T.A.); Grant-in-Aid for Young Scientists (B) 22770036 (to M.E.); and a Grant-in-Aid for 21st Century Circle of Excellence Research, Kyoto University (A14).

1. Srikanth A, Schmid M (2011) Regulation of flowering time: All roads lead to Rome. *Cell Mol Life Sci* 68(12):2013–2037.
2. Quail PH (2002) Phytochrome photosensory signalling networks. *Nat Rev Mol Cell Biol* 3(2):85–93.
3. Cashmore AR, Jarillo JA, Wu YJ, Liu D (1999) Cryptochromes: Blue light receptors for plants and animals. *Science* 284(5415):760–765.
4. Briggs WR, Christie JM (2002) Phototropins 1 and 2: Versatile plant blue-light receptors. *Trends Plant Sci* 7(5):204–210.
5. Imaizumi T, Tran HG, Swartz TE, Briggs WR, Kay SA (2003) FKF1 is essential for photoperiodic-specific light signalling in *Arabidopsis*. *Nature* 426(6964):302–306.
6. Rizzini L, et al. (2011) Perception of UV-B by the *Arabidopsis* UVR8 protein. *Science* 332(6025):103–106.
7. Yanovsky MJ, Kay SA (2002) Molecular basis of seasonal time measurement in *Arabidopsis*. *Nature* 419(6904):308–312.
8. Cerdán PD, Chory J (2003) Regulation of flowering time by light quality. *Nature* 423(6942):881–885.
9. Halliday KJ, Salter MG, Thingnaes E, Whitelam GC (2003) Phytochrome control of flowering is temperature sensitive and correlates with expression of the floral integrator *FT*. *Plant J* 33(5):875–885.
10. Iñigo S, Giraldez AN, Chory J, Cerdán PD (2012) Proteasome-mediated turnover of Arabidopsis MED25 is coupled to the activation of *FLOWERING LOCUS T* transcription. *Plant Physiol* 160(3):1662–1673.
11. Guo H, Yang H, Mockler TC, Lin C (1998) Regulation of flowering time by *Arabidopsis* photoreceptors. *Science* 279(5355):1360–1363.
12. Imaizumi T, Schultz TF, Harmon FG, Ho LA, Kay SA (2005) FKF1 F-box protein mediates cyclic degradation of a repressor of *CONSTANS* in *Arabidopsis*. *Science* 309(5732):293–297.
13. Valverde F, et al. (2004) Photoreceptor regulation of CONSTANS protein in photoperiodic flowering. *Science* 303(5660):1003–1006.
14. Song YH, Smith RW, To BJ, Millar AJ, Imaizumi T (2012) FKF1 conveys timing information for CONSTANS stabilization in photoperiodic flowering. *Science* 336(6084):1045–1049.
15. Lazaro A, Valverde F, Piñeiro M, Jarillo JA (2012) The *Arabidopsis* E3 ubiquitin ligase HOS1 negatively regulates CONSTANS abundance in the photoperiodic control of flowering. *Plant Cell* 24(3):982–999.
16. Zuo Z, Liu H, Liu B, Liu X, Lin C (2011) Blue light-dependent interaction of CRY2 with SPA1 regulates COP1 activity and floral initiation in Arabidopsis. *Curr Biol* 21(10):841–847.
17. Jang S, et al. (2008) *Arabidopsis* COP1 shapes the temporal pattern of CO accumulation conferring a photoperiodic flowering response. *EMBO J* 27(8):1277–1288.
18. Kardailsky I, et al. (1999) Activation tagging of the floral inducer *FT*. *Science* 286(5446):1962–1965.
19. Kobayashi Y, Kaya H, Goto K, Iwabuchi M, Araki T (1999) A pair of related genes with antagonistic roles in mediating flowering signals. *Science* 286(5446):1960–1962.
20. Kobayashi Y, Weigel D (2007) Move on up, it's time for change—Mobile signals controlling photoperiod-dependent flowering. *Genes Dev* 21(19):2371–2384.
21. Michaels SD, Himelblau E, Kim SY, Schomburg FM, Amasino RM (2005) Integration of flowering signals in winter-annual Arabidopsis. *Plant Physiol* 137(1):149–156.
22. Yamaguchi A, Kobayashi Y, Goto K, Abe M, Araki T (2005) *TWIN SISTER OF FT* (*TSF*) acts as a floral pathway integrator redundantly with *FT*. *Plant Cell Physiol* 46(8):1175–1189.
23. Yoo SK, et al. (2005) *CONSTANS* activates *SUPPRESSOR OF OVEREXPRESSION OF CONSTANS 1* through *FLOWERING LOCUS T* to promote flowering in Arabidopsis. *Plant Physiol* 139(2):770–778.
24. Till BJ, et al. (2003) Large-scale discovery of induced point mutations with high-throughput TILLING. *Genome Res* 13(3):524–530.
25. Koornneef M, Hanhart CJ, van der Veen JH (1991) A genetic and physiological analysis of late flowering mutants in *Arabidopsis thaliana*. *Mol Gen Genet* 229(1):57–66.
26. Mockler TC, Guo H, Yang H, Duong H, Lin C (1999) Antagonistic actions of *Arabidopsis* cryptochromes and phytochrome B in the regulation of floral induction. *Development* 126(10):2073–2082.
27. Franklin KA, Larner VS, Whitelam GC (2005) The signal transducing photoreceptors of plants. *Int J Dev Biol* 49(5-6):653–664.
28. Simpson GG, Dean C (2002) *Arabidopsis*, the Rosetta stone of flowering time? *Science* 296(5566):285–289.
29. Wollenberg AC, Strasser B, Cerdán PD, Amasino RM (2008) Acceleration of flowering during shade avoidance in Arabidopsis alters the balance between *FLOWERING LOCUS C*-mediated repression and photoperiodic induction of flowering. *Plant Physiol* 148(3):1681–1694.
30. Yasui Y, et al. (2012) The phytochrome-interacting vascular plant one-zinc finger1 and VOZ2 redundantly regulate flowering in *Arabidopsis*. *Plant Cell* 24(8):3248–3263.
31. Michael TP, et al. (2008) A morning-specific phytohormone gene expression program underlying rhythmic plant growth. *PLoS Biol* 6(9):e225.
32. Yamaguchi R, Nakamura M, Mochizuki N, Kay SA, Nagatani A (1999) Light-dependent translocation of a phytochrome B-GFP fusion protein to the nucleus in transgenic *Arabidopsis*. *J Cell Biol* 145(3):437–445.
33. Kircher S, et al. (1999) Light quality-dependent nuclear import of the plant photoreceptors phytochrome A and B. *Plant Cell* 11(8):1445–1456.
34. Matsushita T, Mochizuki N, Nagatani A (2003) Dimers of the N-terminal domain of phytochrome B are functional in the nucleus. *Nature* 424(6948):571–574.
35. Notaguchi M, et al. (2008) Long-distance, graft-transmissible action of *Arabidopsis* FLOWERING LOCUS T protein to promote flowering. *Plant Cell Physiol* 49(11):1645–1658.
36. Castillon A, Shen H, Huq E (2007) Phytochrome Interacting Factors: Central players in phytochrome-mediated light signaling networks. *Trends Plant Sci* 12(11):514–521.
37. Shin J, et al. (2009) Phytochromes promote seedling light responses by inhibiting four negatively-acting phytochrome-interacting factors. *Proc Natl Acad Sci USA* 106(18):7660–7665.
38. Endo M, Nakamura S, Araki T, Mochizuki N, Nagatani A (2005) Phytochrome B in the mesophyll delays flowering by suppressing *FLOWERING LOCUS T* expression in Arabidopsis vascular bundles. *Plant Cell* 17(7):1941–1952.
39. Endo M, Mochizuki N, Suzuki T, Nagatani A (2007) CRYPTOCHROME2 in vascular bundles regulates flowering in Arabidopsis. *Plant Cell* 19(1):84–93.
40. Kim SY, Yu X, Michaels SD (2008) Regulation of *CONSTANS* and *FLOWERING LOCUS T* expression in response to changing light quality. *Plant Physiol* 148(1):269–279.
41. Bauer D, et al. (2004) Constitutive photomorphogenesis 1 and multiple photoreceptors control degradation of phytochrome interacting factor 3, a transcription factor required for light signaling in Arabidopsis. *Plant Cell* 16(6):1433–1445.
42. Paik I, Yang S, Choi G (2012) Phytochrome regulates translation of mRNA in the cytosol. *Proc Natl Acad Sci USA* 109(4):1335–1340.
43. Wyce A, Henry KW, Berger SL (2004) H2B ubiquitylation and de-ubiquitylation in gene activation. *Novartis Found Symp* 259:63–73; discussion 73–77, 163–169.
44. Sterner DE, et al. (1999) Functional organization of the yeast SAGA complex: Distinct components involved in structural integrity, nucleosome acetylation, and TATA-binding protein interaction. *Mol Cell Biol* 19(1):86–98.
45. Nagy Z, et al. (2009) The human SPT20-containing SAGA complex plays a direct role in the regulation of endoplasmic reticulum stress-induced genes. *Mol Cell Biol* 29(6):1649–1660.
46. Tanese N, Tjian R (1993) Coactivators and TAFs: A new class of eukaryotic transcription factors that connect activators to the basal machinery. *Cold Spring Harb Symp Quant Biol* 58:179–185.
47. Lin J, Handschin C, Spiegelman BM (2005) Metabolic control through the PGC-1 family of transcription coactivators. *Cell Metab* 1(6):361–370.
48. Jang IC, Henriques R, Seo HS, Nagatani A, Chua NH (2010) *Arabidopsis* PHYTOCHROME INTERACTING FACTOR proteins promote phytochrome B polyubiquitination by COP1 E3 ligase in the nucleus. *Plant Cell* 22(7):2370–2383.
49. Betsuyaku S, et al. (2011) Mitogen-activated protein kinase regulated by the CLAVATA receptors contributes to shoot apical meristem homeostasis. *Plant Cell Physiol* 52(1):14–29.